How Does Your Face Change Over Time?

Yifei Sun

Master of Science

Data Science

School of Informatics

University of Edinburgh

2021

Abstract

Face analysis, the basis of many other computer vision tasks, is a popular topic in the computer vision field. Previous studies about facial change analysis covers a longer time range of several years or a shorter time range of several minutes. So there remains a question of how the face changes over several days or months. To address this question, we designed a programme with the function of face detection, face alignment and face change analysis, and get the analysis results of three different participants. The eigenface analysis showed some meaningful eigenfaces to represent the facial changes and the time series analysis found the differences in the face at different times.

Acknowledgements

I would like to thank my supervisor, Prof. Robert Fisher, who generously gives me help and support during the project. I would also like to appreciate support from my family and friends to help me collect data and in all aspects of life.

Declaration

I declare that this thesis was composed by myself, that the work contained herein is my own except where explicitly stated otherwise in the text, and that this work has not been submitted for any other degree or professional qualification except as specified.

(*Yifei Sun*)

Table of Contents

Chapter 1

Introduction

The human face contains abundant information about human behaviour. From the images of face, we can get data of various aspects other than the identity of a person:Facial expressions indicate emotional [1], physiological and pathological conditions [2][3] of people; Facial features reveal the gender and ethic [4] of the face, as well as the age group of the face [5]; Internal facial features are even related to the personality and health [6]. Thus, an increasing number of researchers are concerned about the face, and face analysis becomes popular in the computer vision field.

Face analysis has become a key component in the computer vision field, including face detection, facial expressions analysis, age progression, face recognition and so on. This is because that the applications of face analysis techniques can be used in a wide range. Dabbah et al. [7] represented a technique to implement secure automatic authorization by using the cancellable biometric data. Horng et al. [8] proposed a vision-based real-time driver fatigue detection system to keep safe when driving. Mahajan et al. [9] proposed a face swapping application called SwapItUp to protect privacy.

There are also some scientists caring about the changes in one person's face over a period of time. Ricanek and Boone [10] studied the effect of age progression, which includes both structural and texture changes. Jeong and Finkelstein [11] evaluated the changes of skin colour on face within several minutes by a high speed camera to assess blood pressure. Then here comes the question: How does the facial change in a different time scale, a day or several months?

In this work, we aims to answer the question mentioned above. To be more specific, we aim to figure out the shape and colour changes on one's face in a few months, which focuses on facial features such as the face contour, the skin tone, the colour of

the cheek, the shape of bags under eyes and so on. And try to find out whether the changes in the face have some periodic patterns.

To achieve the goal, we create a programme to implement face detection, face alignment and facial change analysis, which will be discussed in detail in the following chapters. The programme uses real facial images collected from 6 participants who provide images of their face in several months.

1.1 Structure

In Chapter 2, we give an introduction to the background knowledge we used in this work, which including the face alignment techniques and the eigenface method. We also introduce the dataset we collect.

In Chapter 3, we describe the steps we take for preprocessing the image dataset. We follow the order of face alignment, affine transformation and masking to make the images suitable for the eigenface method.

In Chapter 4 and Chapter 5, we show results of eigenface analysis and time series analysis for the face images.

In Chapter 7, we conclude.

Chapter 2

Background

2.1 Face alignment

The aims of face alignment are to find pre-defined facial landmarks on a facial image and map the face to a standard facial image where the size and location of the face are set. Facial landmarks are defined as the predefined points on a face image, which are mainly located around or centred at the important facial features such as eyes, mouth, nose and chin [12].

Face alignment works as the premise for other facial analysis missions including human-computer interaction, face swapping [13] and face animation[14]. Due to the impact of various factors both from outside (e.g. lighting conditions and occlusions) and inside (e.g. gender, age and facial expressions), the face can be extremely different, which makes it a challenging task [15].

Conventional methods for face alignment includes Active Appearance Models (AAM) [16] and Active Shape Model (ASM) [17] are non-rigid face alignment techniques that can be applied to various kinds of faces. Zhao et al. proposed an approach to optimize the AAM subspace model quickly and improve the performance of AAM based face alignment remarkably [18]. Jiao et al. proposed the W-ASM method used Gabor wavelet features to model local image structure, which is capable to align and locate facial features accurately [19]. Wang et al. proposed a face alignment technique combining a variant of the AAM method with an embedded ASM refinement to get effective applications [20].

There are methods combining the face alignment techniques from previous research with deep learning techniques, which relies on the advances both in hardware and optimization techniques. Miao et al. proposed a state-of-the-art method called

the direct shape regression network (DSRN) for end-to-end face alignment by tackling the aforementioned challenges in a unified framework [21]. Shao et al. proposed a multi-center convolutional neural network for unconstrained face alignment and got excellent results on experiments [22].

2.2 Eigenface method

Dealing with the image data is always consuming a large number of computing resources and storage because every pixel in the image is important while analysing. So it is natural to employ dimensionality reduction techniques to reduce the dimension of image data before further analysis. The commonly used method for dimensionality reduction is principal components analysis (PCA) [23], especially in some computer vision tasks such as face recognition [24].

The core idea of PCA is to choose an optimal subspace with reduced dimensions where keeps as much variation as possible of the original dataset. To give clear explanation [25], we assume a set of l-dimensional data vector $X = \{x_p\}$, $p \in \{1,...,N\}$ is reduced to a set of m-dimensional feature vector $S = \{s_p\}$, $p \in \{1,...,N\}$ by a transformation matrix W as follow:

$$s_p = W^{\mathrm{T}}(x_p - m) \tag{2.1}$$

where m, $m = \frac{1}{N}\sum_{p=1}^{N} x_p$, $W = (w_1,...,w_m)$ and the vector w_j is the eigenvector of the jth largest eigenvalue of the covariance matrix:

$$C = \frac{1}{N}\sum_{p=1}^{N}(x_p - m)(x_p - m)^{\mathrm{T}} \tag{2.2}$$

satisfying $Cw_k = \lambda_k w_k$. The m principal axes in W are orthonormal axes onto which the retained variance under projection is maximal.

When we employ PCA to face images, the eigenvectors are known as eigenfaces. Since Turk and Pentland [26] proposed an eigenfaces method for face recognition, it is widely used in this area. Agarwal et al. proposed a face recognition method combining the eigenface method and artificial neural network (ANN) and achieved a recognition rate of 97.018%

2.3 Dataset

We have six datasets in total, each of which is consists of the face images of a participant. And the detailed information of the datasets is listed below.

- Participant 1: The participant takes four pictures of her face at 10:00, 14:00, 20:00 and 24:00 everyday. We get 110 face images of this participant at each time, and the dataset of participant 1 is consists of 440 face images in total. The background and lighting conditions of the images vary in different images. The device used for collecting the images is an iPhone 11.

- Participant 2: The participant takes one picture of her face at 19:00 everyday. The dataset of participant 2 is consists of 100 face images in total. The images can be divided into two groups: taken in the same room and taken in outdoors. The device used for collecting the images is a HUAWEI Mate 20.

- Participant 3: The participant takes pictures of his face at a different time everyday, and the time is in a wide range from 7:00 am to 3:00 am. The dataset of participant 3 is consists of 154 face images in total. The images are always taken in the same room. The device used for collecting the images is a Samsung Galaxy A40.

- Participant 4, 5 and 6: These participants take one picture of their face at around 24:00 everyday. Since the number of images is less than 100 for each participant and the time stays the same, we do not use these images for further analysis. The devices used for collecting the images are a Vivo X30 Pro, an iPhone 11 and an iPhone Xs Max .

Chapter 3

Pre-processing

The eigenface approach used in this project is based on the PCA algorithm, which means it takes every pixel in the images into account to find the eigenfaces. When focusing on the shape and colour changes on one's face, the eigenfaces should represent these changes rather than the differences in the background or position of the faces in the images.

In that case, it is important to remove irrelevant factors in the images. Though the participants are asked to take their pictures every day under the same condition, there will still be some unrelated variations in the images that affect the analysis, such as illumination conditions, pose variations and unexpected occlusions.

3.1 Face Alignment

3.1.1 Methodology

To remove the influence of the face position in an image, I aligned the images from the same participant to a common coordinate system. Since the dataset is consists of images of participants, there is only one face in the centre of each image.

The face detector and pre-trained feature predictor from Dlib are used in the face alignment step. Dlib [27] is an open source library written in C++, which is used in various platform including python. It has a variety of software components to address different kinds of challenges such as image processing, machine learning, data mining and many other difficult tasks. The Dlib software toolkit provides tools for detecting various kinds of objects in images and also a frontal face detector for detecting human faces that are facing the camera.

This face detector in Dlib is based on the classic Histogram of Oriented Gradients (HOG) feature combined with a linear classifier, an image pyramid, and a sliding window detection scheme [27]. The detector is general and able to detect many types of semi-rigid objects other than human faces. HOG descriptors were first applied to the computer vision field in 2005 [28] when Dalal and Triggs used the descriptors combined with a linear SVM classifier to detect pedestrians in static images or videos. In the key thought of HOG, the appearance and shape of a local object in an image can be described by the distribution of intensity gradients or edge directions. By dividing the image into small connected regions which are called cells, each cell can generate a histogram of gradient directions according to the pixels in the cell. And these histograms form the HOG descriptor. It is invariant to illumination or geometry changes, thus, it is suitable for human detection.

After getting a bounding box by the face detector, the shape predictor with a pre-trained model of 68 face landmarks (as shown by red dots in Figure 3.1 a) will predict the face landmark positions to detect facial features.

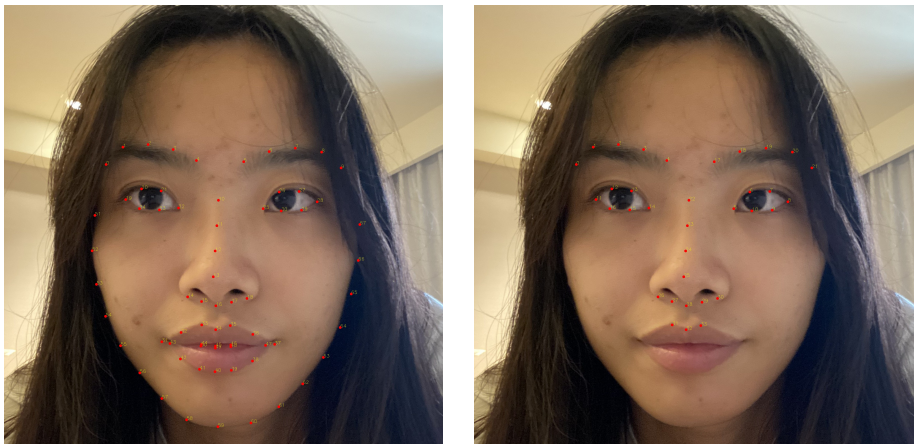

(a) 68 facial landmarks (b) landmarks used for alignment

Figure 3.1: Facial Landmarks

As shown by red dots in Figure 3.1 b, the facial landmarks I choose for face alignment are 34 points which represent the location of both eyes, both eyebrows, nose and the top of the upper lip. This is due to the factor that the participants have a slight variance in their expressions when they take the pictures, which will cause the movement of the corner of the mouth and eyeballs. The location of these fiducial points is stable as the expressions change. These points are used to align the faces from the same participant to the common coordinate system by the affine transformation.

Affine transformation [29] is any combination of basic 2D transformations includ-

ing translations, rotations, dilations and shears, which preserves collinearity and ratio of distances. In geometry, affine transformation means that a vector space is transformed into another vector space by a linear transformation followed by a translation. Affine transformations can be represented as a matrix:

$$\begin{pmatrix} x \\ y \end{pmatrix} = \begin{pmatrix} m_1 & m_2 \\ m_3 & m_4 \end{pmatrix} \begin{pmatrix} \hat{x} \\ \hat{y} \end{pmatrix} + \begin{pmatrix} t_1 \\ t_2 \end{pmatrix} \tag{3.1}$$

Eq 4.1 can be written as:

$$\mathbf{x}'_i = \mathbf{M}\mathbf{x}_i + \mathbf{t} \tag{3.2}$$

where

$$\mathbf{M} = \begin{pmatrix} m_1 & m_2 \\ m_3 & m_4 \end{pmatrix} \tag{3.3}$$

Given the target images and original images, we can get the affine transformation matrix M by minimizing:

$$\sum_{i=1}^{n} \left\| \mathbf{x}'_i - \mathbf{M}\mathbf{x}_i - \mathbf{t} \right\|^2 \tag{3.4}$$

3.1.2 Evaluation

To evaluate the performance of the face alignment code, I find some features on each participant's face and compare the location of these features in the images after alignment. I set a small box around the feature and use the grey centroid method [30] to find the location of the feature. The features I use are moles or acne scars on the face, so they are always the darkest part within the box I set, which is also the grey centroid of the patch.

For the image shown in Figure 3.2, the white point is the grey centroid of the patch in the white box.

The coordinate of grey (intensity) centroid can be computed as follow:

$$\begin{aligned} x &= \textstyle\sum_I^{M\times N} i \cdot I(x,y) / \sum_I^{M\times N} I(x,y) \\ y &= \textstyle\sum_I^{M\times N} j \cdot I(x,y) / \sum_I^{M\times N} I(x,y) \end{aligned} \tag{3.5}$$

where $I(x,y)$ stands for the grey intensity value of the pixel (x,y). M and N is the width and height of the patch. The size of the patches used in this project is 20*20 pixels.

The results of grey centroids of chosen feature areas on each participants' face are shown in Figure 3.3, where p1, p2, p3 stands for three different participants respectively.

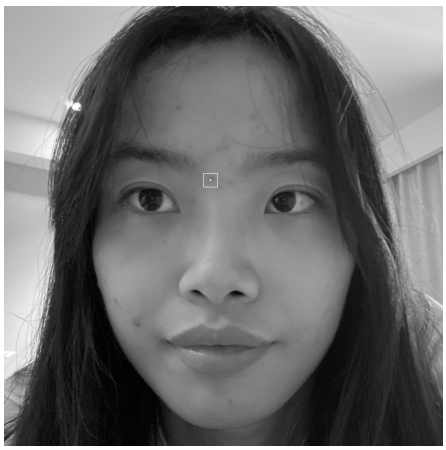

Figure 3.2: A grey scale image after alignment

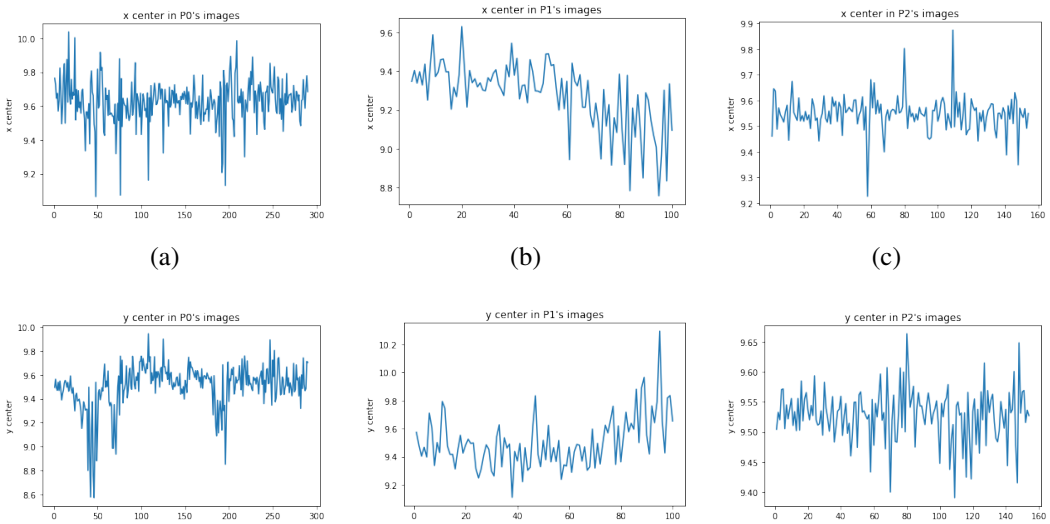

(a) (b) (c)

(d) (e) (f)

Figure 3.3: Grey centroid

The mean values and standard deviations of the grey centroid's coordination are shown in table 3.1. The table and plots show that the locations of the grey centroids have a tight average with a small standard deviation in every dataset. And the standard deviations are around 0.1 pixel, which means the face alignment method can be used in this project.

3.2 Remove Other Irrelevant Factors

As mentioned before, there are variables in the image caused by the background. To remove the influence of background, we can mask the image to focus on the area we

	x center		y center	
	mean	dev	mean	dev
P1	9.63	0.13	9.50	0.18
P2	9.28	0.17	9.33	0.17
P3	9.54	0.07	9.53	0.04

Table 3.1: The mean value and standard deviation of grey centroid's coordinate

are interested in. Masking is to use the select image, figure or object to block the image to control the interesting area, and the specific image used for coverage is called a mask.

As shown in Figure 3.4, the mask covers the area of background and the lower jaw which will change slightly when the expressions change. There will be a different mask for each participant based on the facial features they have. For example, the participant in Figure 3.5 has a moustache that has a different length in each image, so the masking should also cover this part of the face.

After masking, the pre-processing steps of the images are done and the images are ready for the eigenface method (as described in the next chapter).

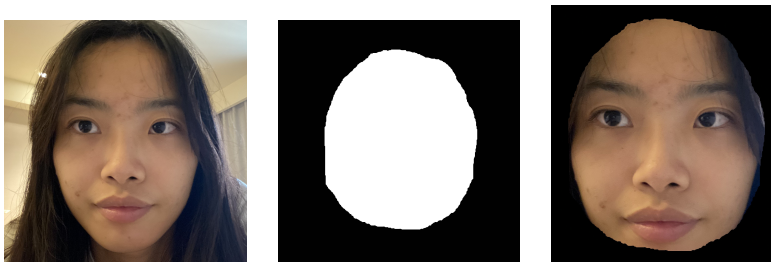

(a) Original image (b) Mask (c) After masking

Figure 3.4: Masking

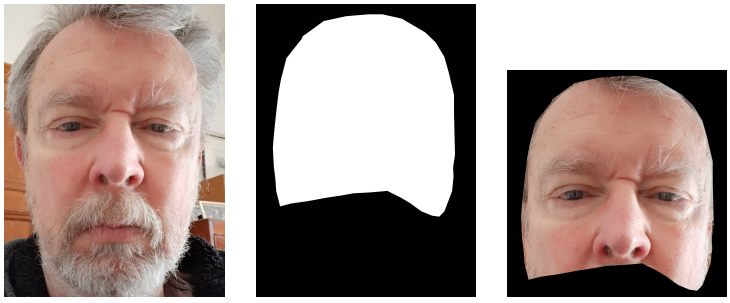

(a) Original image (b) Mask (c) After masking

Figure 3.5: Masking

Chapter 4

Eigenface Analysis

In this section, we want to find a proper way to represent the changes on the faces efficiently, that is, to use the eigenface method [31] based on PCA to extract the relevant information in a face image. The process of the eigenface method is shown in Figure 4.1.

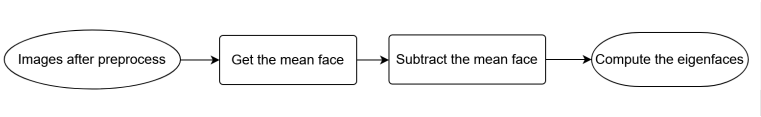

Figure 4.1: The process of computing eigenfaces

In the eigenface method, we try to find the principal components (also known as the eigenvector of the covariance matrix) of the distribution of a set of face images. These eigenvectors are ordered by the variance which means the top-ranked eigenvectors account for more variance among the images than others. Each face image can be projected to the space of eigenfaces as a linear combination of the eigenfaces as shown in Figure 5.11.

Figure 4.2: Projection a face to space of eigenfaces

For a greyscale face image in the size of M*N pixels, it can be considered as a vector of dimension M*N. Then each image can be considered as a point in M*N dimensional space. And the dimension becomes 3*M*N when dealing with colour

images because each pixel in the colour image has three values associated with RGB channels. In that way, we map a set of face images to a set of points in the high dimensional space. Similar to other datasets with a high dimension, the face images are not randomly distributed in the high dimensional space and can be approximately described in a low dimensional subspace where the number of dimensions is relatively lower than M*N. To choose the number of dimensions, K, we combine the cumulative explained variance ratio plot (Figure 4.3 a) and the scree plot (Figure 4.3 b) for eigenvalue. The explained variance ratio here accounts for the ratio of the eigenvalue of its eigenvector to the sum of all eigenvalues, which can be translated as how important the eigenvector is among all. We set a threshold value of 0.9 for the cumulative explained variance ratio and find the points where the rate of decline changes the most in the scree plots.

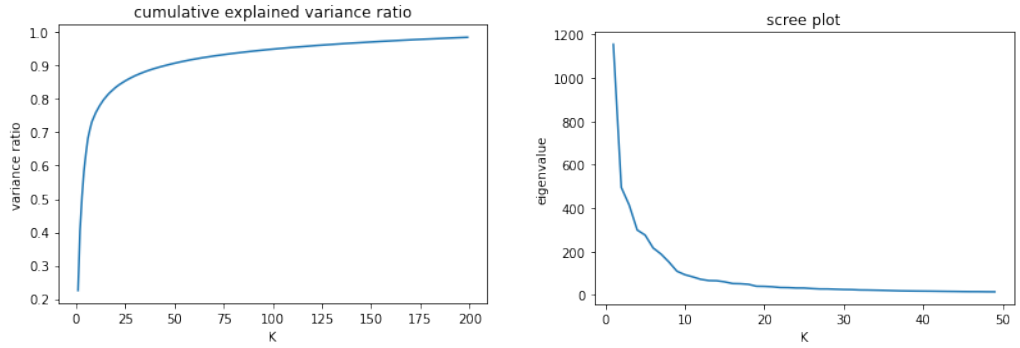

(a) (b)

Figure 4.3: How to pick K

4.1 Greyscale Images

We try to find the changes on the face images both in shape and colour. When focusing on the shape changes, we can apply the eigenface method on the greyscale images which can not reflect the colour changes. However, the greyscale images preserve the brightness information while discarding the saturation and hue information.

4.1.1 Participant 1

By combining the cumulative explained variance ratio plot and the scree plot for eigenvalue, we decide to use K=25 eigenfaces to describe the face images of participant 1.

The average face and the first 25 eigenfaces (also means the most important eigenfaces) are shown in Figure 4.4 a and Figure 4.4 b respectively.

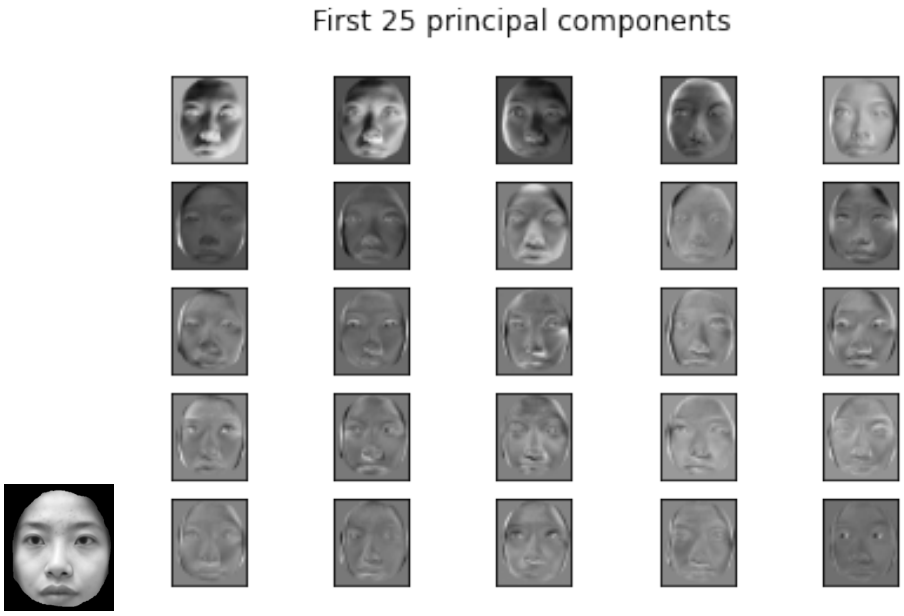

(a) (b)

Figure 4.4: Eigenfaces of participant 1

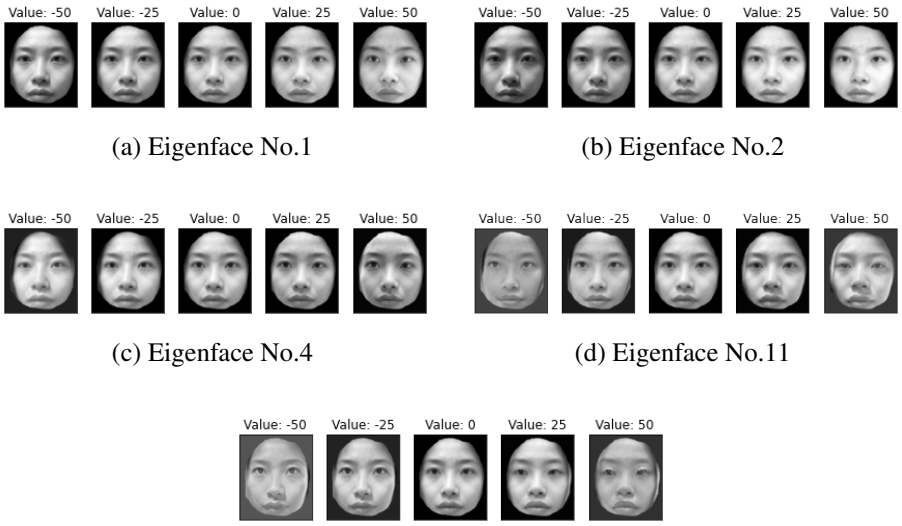

(a) Eigenface No.1

(b) Eigenface No.2

(c) Eigenface No.4

(d) Eigenface No.11

(e) Eigenface No.12

Figure 4.5: Some special Eigenfaces of participant 1

In order to find some eigenfaces that are related to the shape changes on the face and to reveal the meanings and influences of these eigenfaces, we add each eigenface to the average face to see the changes on the face. In Figure 4.5, there are results of

five interesting eigenfaces among all where the values above the images indicate how many times we add the eigenface to the average face. The eigenface in (a) is related to the width of the face: As the value of stack folds increases, the cheek on the left becomes wider. (b) shows the variance in the puffiness under the eyes, while (c) shows the difference in two nasolabial folds, also, a more defined face appears at the value of -50 while the face at +50 is smoother. In (d), the eyes in the images on the right are more swollen than those on the left, which makes the face looks more tired at +50. In (e), the face cheek on the right becomes bigger as the value of stack folds increases.

4.1.2 Participant 2

Following the same rule to pick K, we decide K=25 for this image dataset of participant 2. The average face and the first 25 eigenfaces are shown in Figure 4.6.

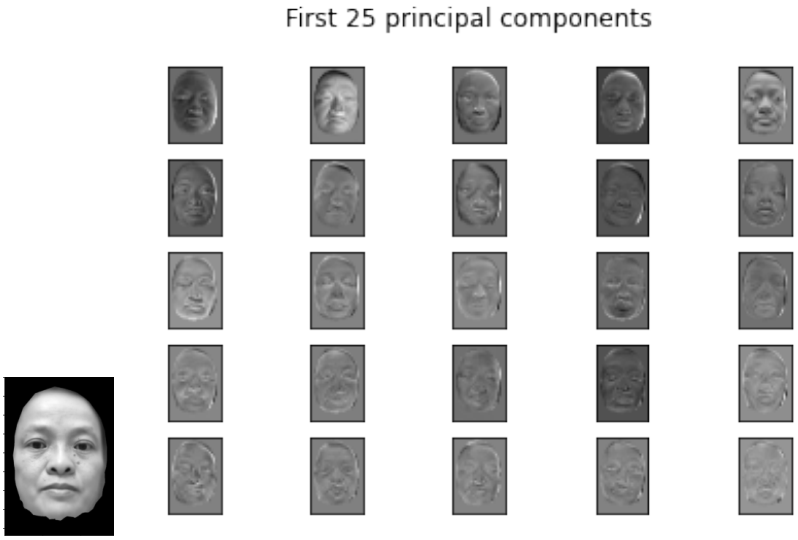

(a) (b)

Figure 4.6: Eigenfaces of participant 2

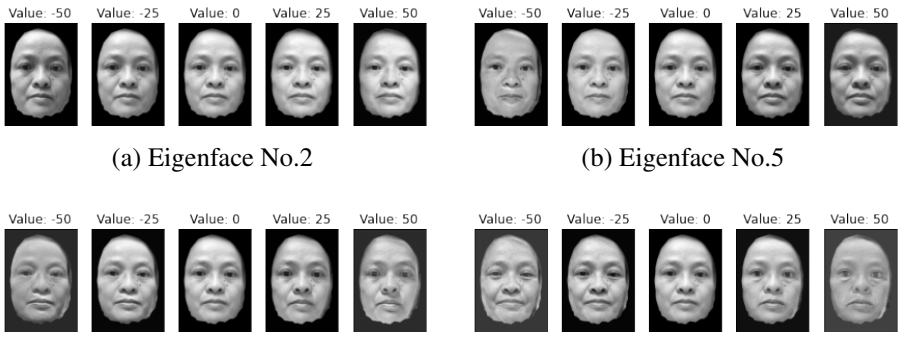

(a) Eigenface No.2 (b) Eigenface No.5

(c) Eigenface No.11 (d) Eigenface No.16

Figure 4.7: Some special Eigenfaces of participant 2

In Figure 4.7, there are results of some important eigenfaces for this dataset. The No.2 eigenface accounts for the difference in the shadow on the face. In (a), there is more shadow on the face at the value of -50, which makes the wrinkles on the face look clearer. The eigenface in (b) represents the different width of the face, and the face on the left is narrower than those on the right. (c) shows the variation of the upper eyelids, and the double eyelid is more defined at +50. The No.16 eigenface makes eyes differ in size. Besides, the face at -50 in (d) is more likely a smiling face, which is also the function of eigenface No.16.

4.1.3 Participant 3

We decide to use K=20 eigenfaces to describe the face images of participant 3. The average face (Figure 4.8 a) and the first 20 eigenfaces (Figure 4.8 b) are shown below.

Figure 4.9 shows some meaningful eigenfaces for the dataset of participant 3. The eigenface in (a) explains the degree of wrinkles on the face, which means that bigger weights of eigenface No.3 lead to deep frowns on the brow. Eigenface No.5 shows the contrast of the face. The face at +50 is more defined in (b). The eigenfaces in (c) and (d) are both related to the size of the eyes on the face. However, eigenface No.7 also works on the bright spot on the nose which can be found easily on the face at 50. And in (d), the face at -50 has deep and big eyes compared with those at bigger values.

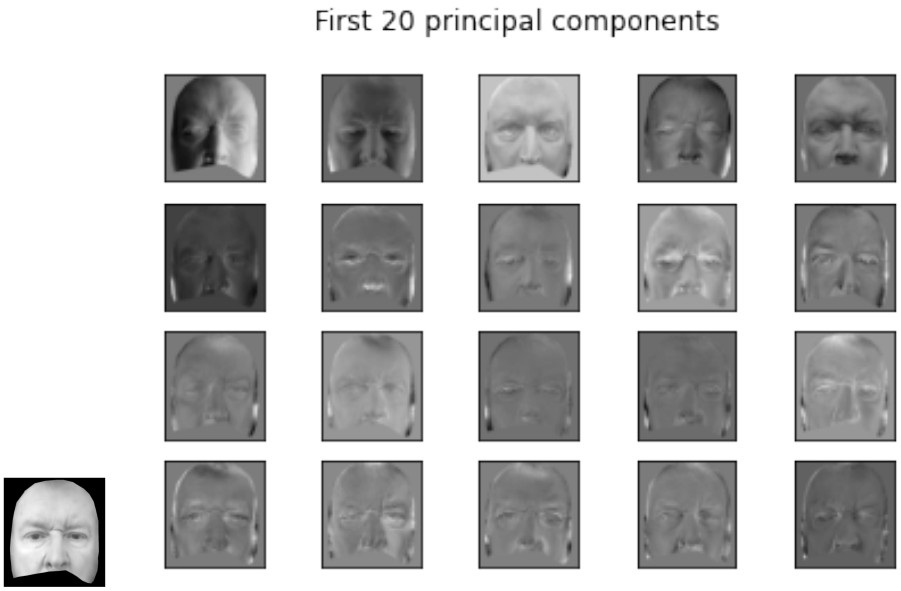

(a) (b)

Figure 4.8: Eigenfaces of participant 3

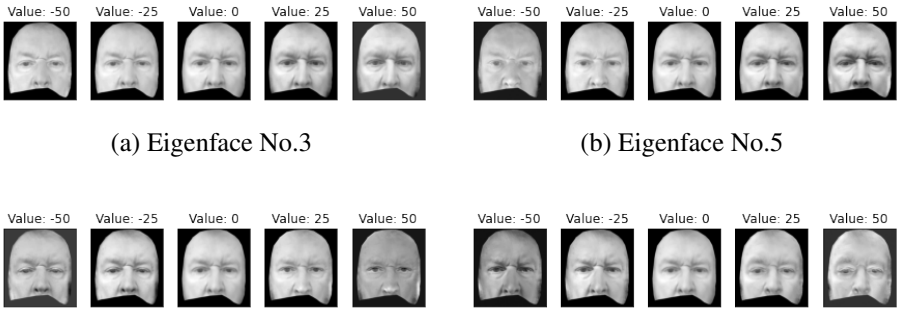

(a) Eigenface No.3 (b) Eigenface No.5

(c) Eigenface No.7 (d) Eigenface No.9

Figure 4.9: Some special Eigenfaces of participant 3

4.2 Colour Images

In this section, we will apply the eigenface method on colour images to find more changes except for the shape changes in the face images. Since colour images have three channels, the vector space they form is three times big as that of greyscale images.

4.2.1 Participant 1

According to the cumulative explained variance ratio plot and the scree plot for eigenvalue, we decide to use K=40 eigenfaces to describe the face images of participant 1.

In Figure 4.10, there are results of four interesting eigenfaces among all.

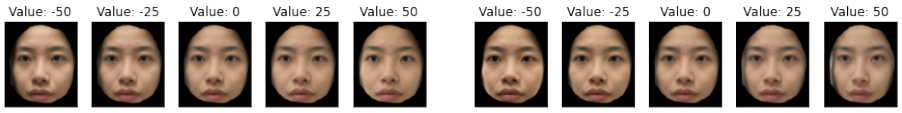

(a) Eigenface No.3

(b) Eigenface No.7

(c) Eigenface No.12

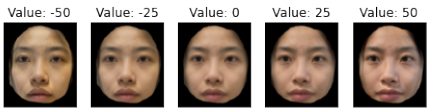

(d) Eigenface No.18

Figure 4.10: Some special Eigenfaces of participant 1

The No.3 eigenface in (a) accounts for the dark circles under the eyes, subtracting the eigenface leads to obvious dark circles. (b) shows the difference in skin tone: With a large value of stack folds, the face looks pale. In (c), the faces on the right are puffier than those on the left. (d) also shows differences in skin colour, but the No.18 eigenface is related to whether the face is rosy.

4.2.2 Participant 2

For these colour images of participant 2, we choose K=40 eigenfaces in this part of the experiment. Figure 4.11 shows eigenfaces with some attractive functions.

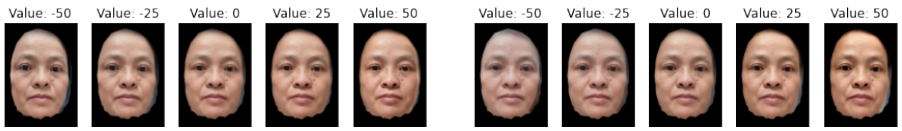

(a) Eigenface No.6

(b) Eigenface No.7

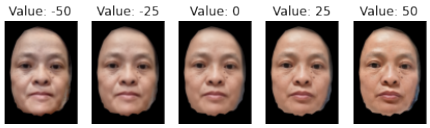

(c) Eigenface No.14

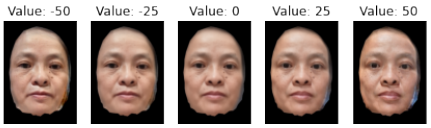

(d) Eigenface No.23

Figure 4.11: Some special Eigenfaces of participant 2

In Figure 4.11, there are results of some important eigenfaces for this dataset. In (a), the face at the value of -50 is lighter and narrower, while the face at +50 is darker and wider. The eigenface in (b) shows the difference in skin colour. The eigenface

No.14 works on the sharpness of facial features, so that, face with a negative weight of this eigenface has a more flat nose, mouth and eyes. The No.23 eigenface is related to how thin the face is. The face at +50 in (d) is obviously thinner than the face at -50, not only because of the difference in face width but also the shape of facial muscles.

4.2.3 Participant 3

For the images of participant 3, the number of dimensions is 30. Among the 30 eigenfaces describing the faces, there are four special eigenfaces with different functions. In Figure 4.12 a, the colour of skin changes from rosy to pale as the weight of eigenface No.9 increases. The eigenface in (b) seems to have some effect on the softness of the face. The face at +50 looks younger than the face at -50. (c) shows the colour change of the red areas on the cheek. The cheek is redder with a bigger weight of eigenface No.24. Eigenface No.30 is related to the red areas on the face as well. However, it controls bigger area than eigenface No.24 does. It can tell from (d) that the weight of this eigenface influences the red areas on the cheek, nose and forehead.

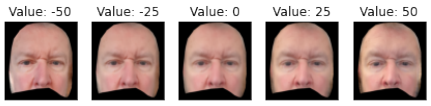

(a) Eigenface No.9

(b) Eigenface No.13

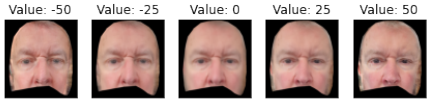

(c) Eigenface No.24

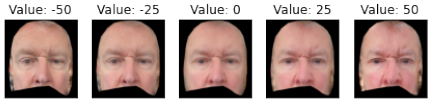

(d) Eigenface No.30

Figure 4.12: Some special Eigenfaces of participant 3

4.3 Summary

According to the eigenfaces we get, we can conclude that:

- The mean face of each participant seems to be clear and not blurry, and it is the same for the mean face after adding some eigenface. So the face alignment function we realize seems to be good enough to be able to use the eigenface method.

- The eigenface method seems to extract a small number of significant eigenfaces. Some of these eigenfaces seem to be related to general face shape and colour, and others to changes in specific features (e.g. eyes, smiles).

Chapter 5

Time Series Analysis

In this section, we try to find some patterns in the changes on the face according to the meaningful eigenfaces we find in the last chapter. As mentioned before, when we project the face images to the space formed by eigenfaces, there are weights of each eigenface to describe each face image. Then we will analyse them in the course of several months and a day to find the change patterns.

5.1 Participant 1

The images of participant 1 are taken at four different times everyday, so we try to make plots about how the mean weights of eigenfaces of different times change in a months. And we also try to find out the changes within a day.

Figure 5.1 and Figure 5.2 shows how the weights of the eigenfaces in Figure 4.5 and Figure 4.10 change in a month.

In Figure 4.5 d, we find the No.11 eigenface is related to the puffiness of eyes, and the larger weight of this eigenface means the puffier the eyes are. Table 5.1 shows the mean value and standard deviation of the weights. It is obvious that the weights in the morning are larger than those for other times of day. And it is compatible with common sense that people get puffy eyes when they get up in the morning.

In Figure 4.10 d, the eigenface accounts for how rosy the face is, and larger weights stand for a rosier face. Table 5.2 shows the mean value and dev of the weights. We can tell that the face is usually rosier at night.

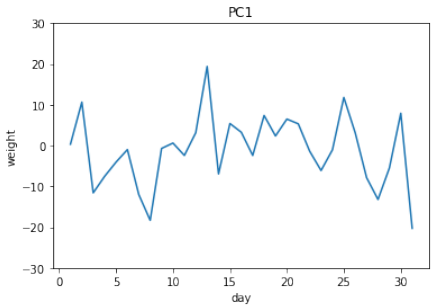

(a) Eigenface No.1

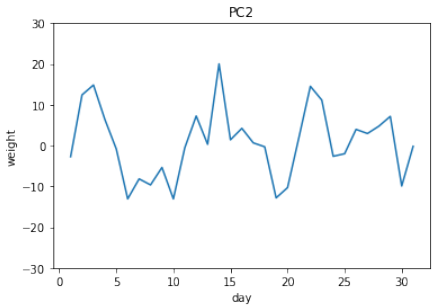

(b) Eigenface No.2

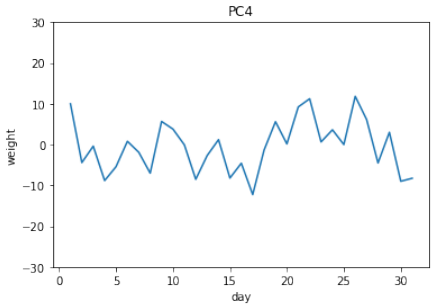

(c) Eigenface No.4

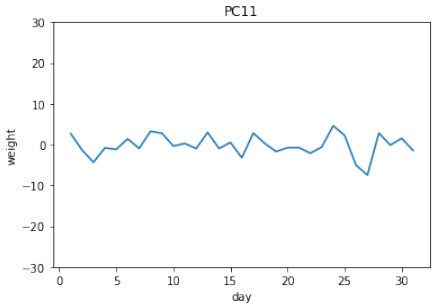

(d) Eigenface No.11

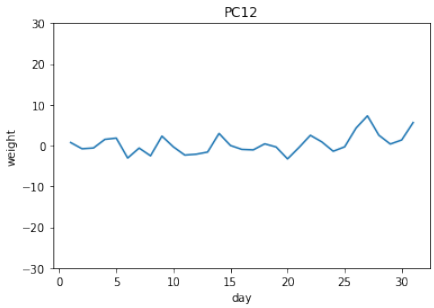

(e) Eigenface No.12

Figure 5.1: Weights of eigenfaces of p1 in Figure 4.5

	Morning (10:00)	Afternoon (14:00)	Evening (20:00)	Midnight (24:00)
	116 pics	116 pics	109 pics	110 pics
mean	2.13	0.12	-1.31	-1.83
dev	3.75	4.48	5.10	3.79

Table 5.1: Weights of No.11 eigenface of p1 at different times of day

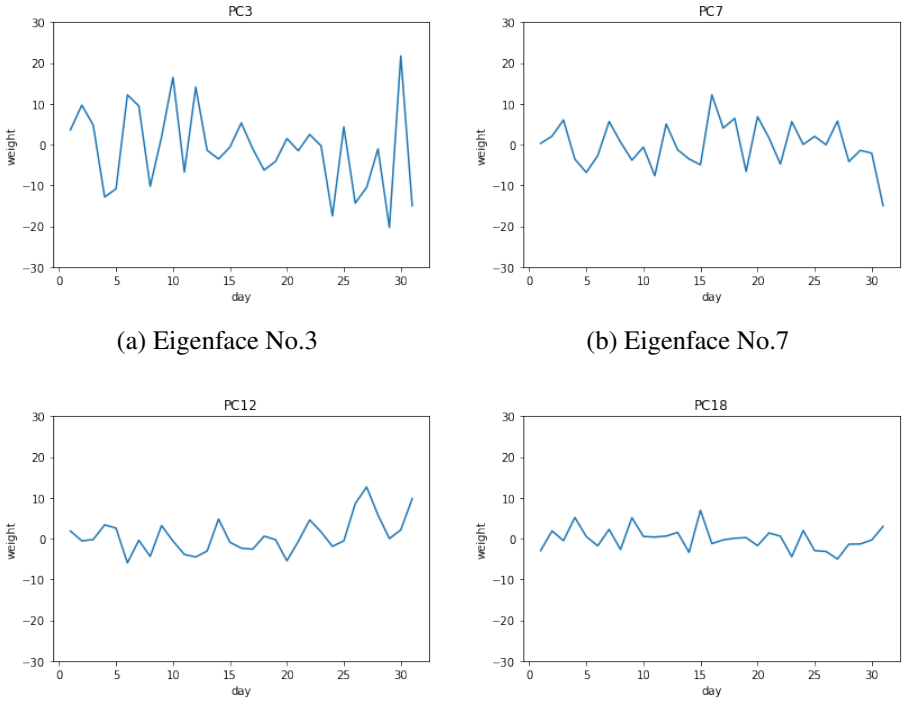

(a) Eigenface No.3

(b) Eigenface No.7

(c) Eigenface No.12

(d) Eigenface No.18

Figure 5.2: Weights of eigenfaces of p1 in Figure 4.10

5.2 Participant 2

The images of participant 2 are taken at the same time everyday, so it is impossible to find the change patterns within a day. The following plots show the weights of some eigenfaces we find in Figure 4.7 and Figure 4.11. The plots in Figure 5.5 represent the weights of the four eigenfaces in Figure 4.5 for 100 days. The plots in Figure 5.6 show the weights of the four eigenfaces in Figure 4.11. However, there is no periodic pattern in them. How the weights of these eigenfaces vary in a month is shown in Figure 5.3 and Figure 5.4. We notice that eigenfaces with large order numbers will usually have small weights.

	Morning (10:00)	Afternoon (14:00)	Evening (20:00)	Midnight (24:00)
	116 pics	116 pics	109 pics	110 pics
mean	-0.74	-0.73	-0.17	1.50
dev	5.53	5.37	4.81	4.59

Table 5.2: Weights of No.18 eigenface of p1 at different times of day

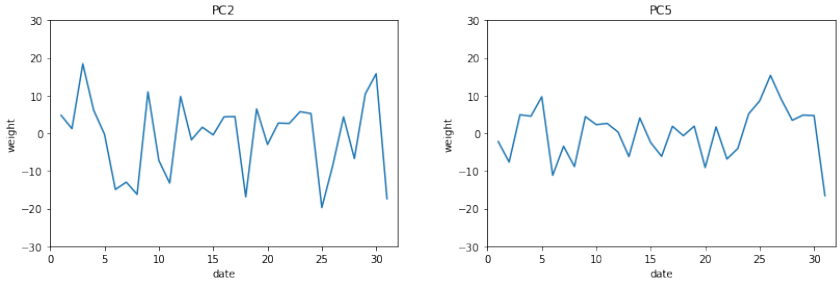

(a) Eigenface No.2 (b) Eigenface No.5

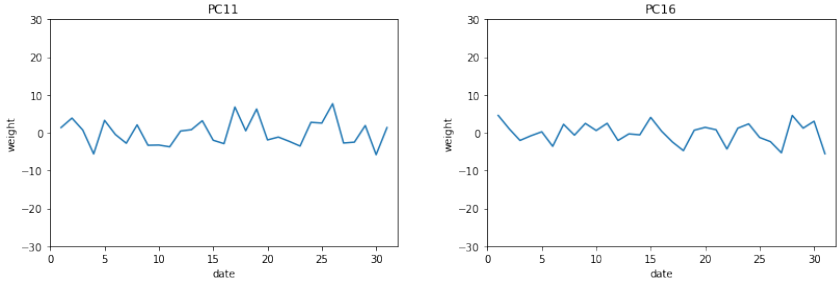

(c) Eigenface No.11 (d) Eigenface No.16

Figure 5.3: Weights of eigenfaces of p2 in Figure 4.7 in a month

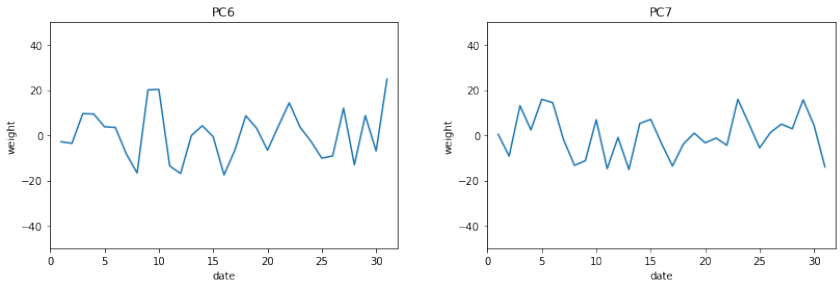

(a) Eigenface No.6 (b) Eigenface No.7

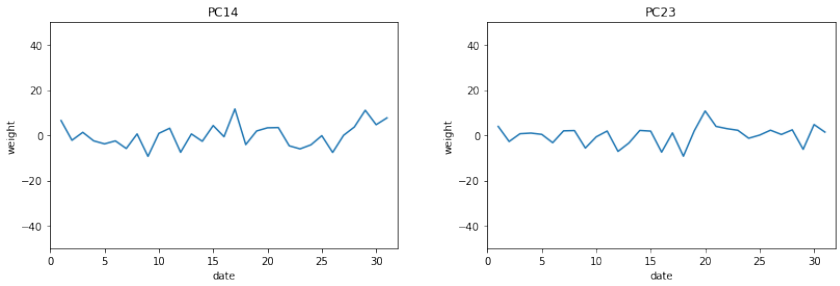

(c) Eigenface No.14 (d) Eigenface No.23

Figure 5.4: Weights of eigenfaces of p2 in Figure 4.11 in a month

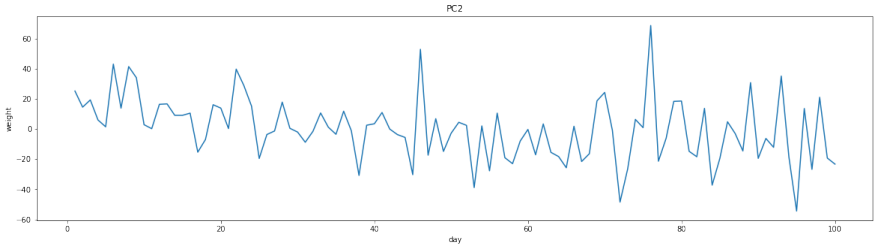

(a) Eigenface No.2

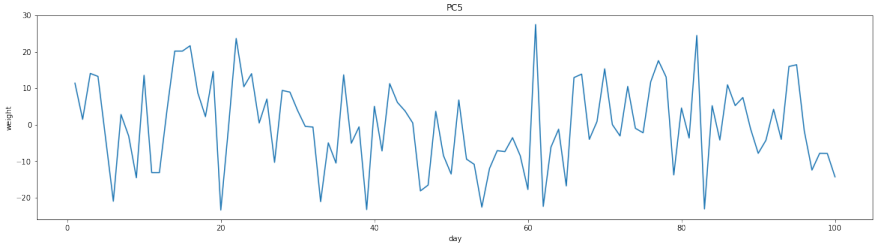

(b) Eigenface No.5

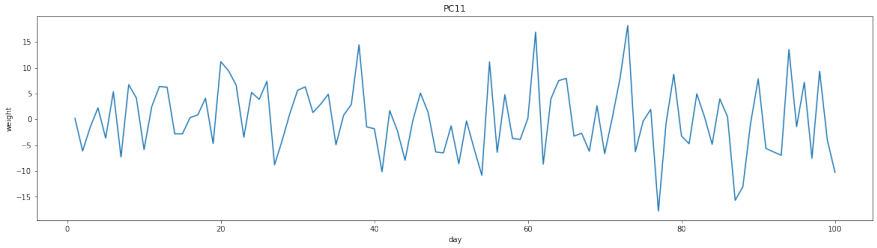

(c) Eigenface No.11

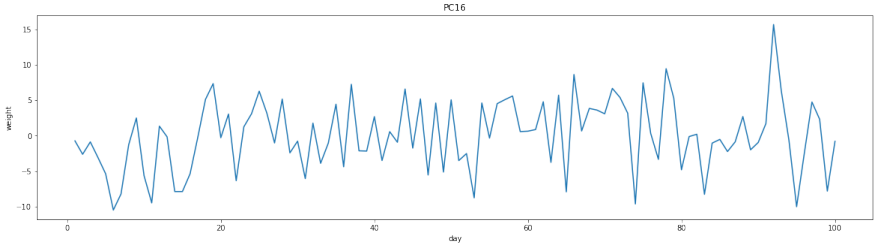

(d) Eigenface No.16

Figure 5.5: Weights of four eigenfaces of p2 in Figure 4.7

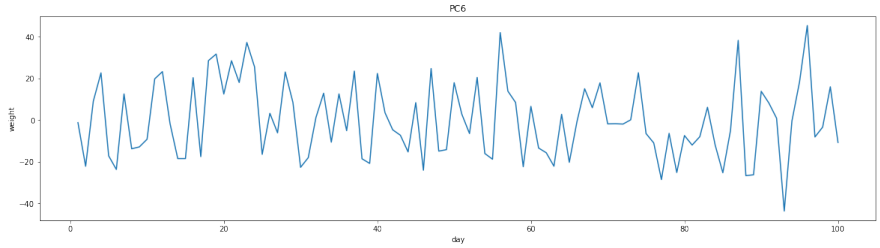

(a) Eigenface No.6

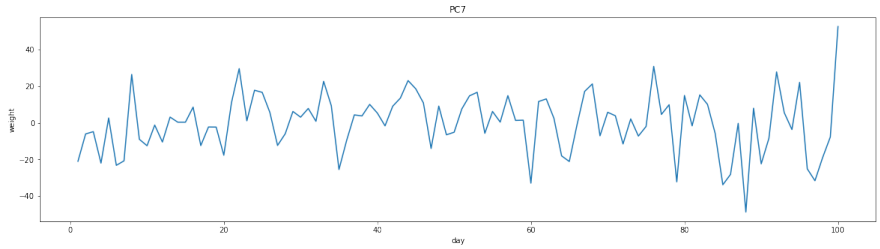

(b) Eigenface No.7

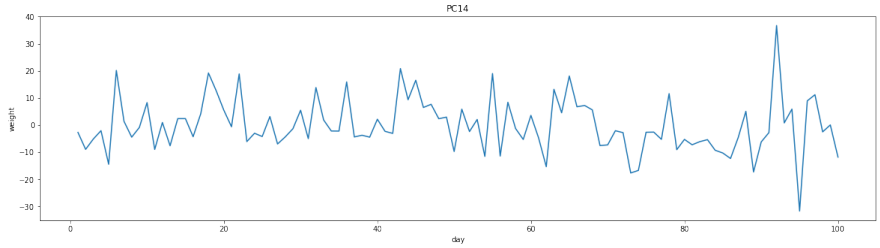

(c) Eigenface No.14

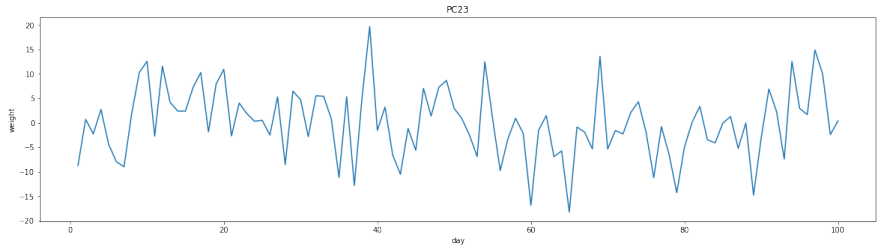

(d) Eigenface No.23

Figure 5.6: Weights of four eigenfaces of p2 in Figure 4.11

5.3 Participant 3

The images of participant 3 are taken at different times everyday, so we try to make plots about how the mean weights of eigenfaces (specified in Figure 4.12) of different times change in three months (shown in Figure 5.9). And we also make plots to figure out how the mean weights of eigenfaces vary in a month by combining the data of three months (shown in Figure 5.7). And Figure 5.10 and Figure 5.8 are the results of eigenfaces in Figure 4.12. However, it is hard to find any periodic patterns on the plots.

Table 5.3, Table 5.4, Table 5.5 and Table 5.6 show the mean values and standard deviations of the weights of the four eigenfaces in Figure 4.12 at different times. From the data listed in the tables, we can assume that the face of participant 3 looks younger during the daytime compared to the face at night. The red areas on participant 3's face are darker in the morning and in the evening compared to the colour of them in the afternoon and midnight.

Table 5.7, Table 5.8, Table 5.9 and Table 5.10 show the mean values and standard deviations of the weights of the four eigenfaces in Figure 4.9 at different times. According to the tables, it seems that the wrinkles are deepened as time passing.

	Morning (7:00-12:00) 64 pics	Afternoon (12:00-18:00) 35 pics	Evening (18:00-24:00) 35 pics	Midnight (after 0:00) 20 pics
mean	-3.15	-0.99	8.28	4.26
dev	11.58	10.39	12.04	14.84

Table 5.3: The mean and dev of weights for eigenface No.9 of p3

	Morning (7:00-12:00) 64 pics	Afternoon (12:00-18:00) 35 pics	Evening (18:00-24:00) 35 pics	Midnight (after 0:00) 20 pics
mean	0.23	0.64	-1.04	-1.29
dev	7.65	9.58	7.24	9.41

Table 5.4: The mean and dev of weights for eigenface No.13 of p3

	Morning (7:00-12:00) 64 pics	Afternoon (12:00-18:00) 35 pics	Evening (18:00-24:00) 35 pics	Midnight (after 0:00) 20 pics
mean	0.36	-0.61	0.64	-0.26
dev	5.46	5.93	5.74	6.56

Table 5.5: The mean and dev of weights for eigenface No.24 of p3

	Morning (7:00-12:00) 64 pics	Afternoon (12:00-18:00) 35 pics	Evening (18:00-24:00) 35 pics	Midnight (after 0:00) 20 pics
mean	1.30	-1.60	0.37	-0.52
dev	4.33	5.71	4.86	4.90

Table 5.6: The mean and dev of weights for eigenface No.30 of p3

	Morning (7:00-12:00) 64 pics	Afternoon (12:00-18:00) 35 pics	Evening (18:00-24:00) 35 pics	Midnight (after 0:00) 20 pics
mean	-1.99	-1.32	3.32	6.36
dev	10.12	11.53	13.87	16.86

Table 5.7: The mean and dev of weights for eigenface No.3 of p3

	Morning (7:00-12:00) 64 pics	Afternoon (12:00-18:00) 35 pics	Evening (18:00-24:00) 35 pics	Midnight (after 0:00) 20 pics
mean	-0.26	-0.29	0.52	1.05
dev	8.78	10.54	9.60	11.23

Table 5.8: The mean and dev of weights for eigenface No.5 of p3

	Morning (7:00-12:00) 64 pics	Afternoon (12:00-18:00) 35 pics	Evening (18:00-24:00) 35 pics	Midnight (after 0:00) 20 pics
mean	-1.07	0.30	-1.73	4.41
dev	6.27	8.95	9.90	9.52

Table 5.9: The mean and dev of weights for eigenface No.7 of p3

	Morning (7:00-12:00) 64 pics	Afternoon (12:00-18:00) 35 pics	Evening (18:00-24:00) 35 pics	Midnight (after 0:00) 20 pics
mean	-1.87	-0.93	5.50	2.79
dev	5.07	5.49	5.85	9.06

Table 5.10: The mean and dev of weights for eigenface No.9 of p3

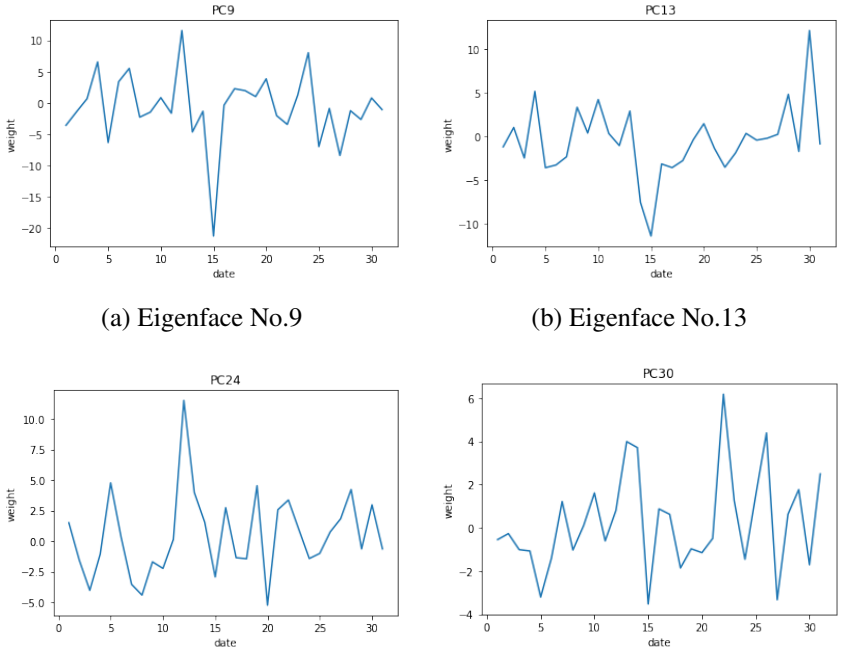

(a) Eigenface No.9

(b) Eigenface No.13

(c) Eigenface No.24

(d) Eigenface No.30

Figure 5.7: Weights of four eigenfaces of p3 in Figure 4.12

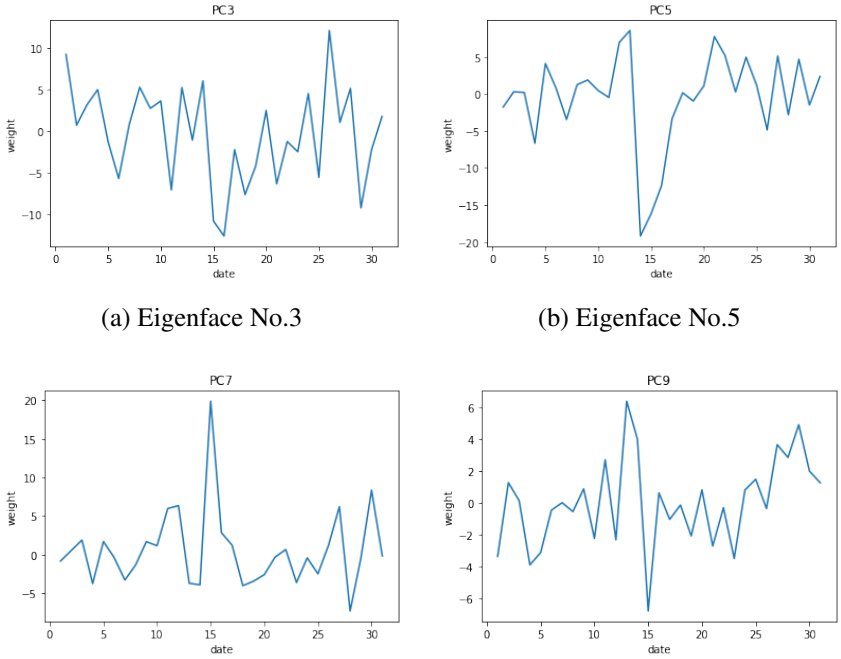

(a) Eigenface No.3

(b) Eigenface No.5

(c) Eigenface No.7

(d) Eigenface No.9

Figure 5.8: Weights of four eigenfaces of p3 in Figure 4.9

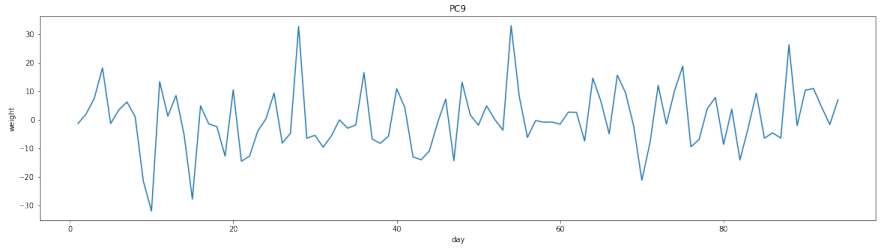

(a) Eigenface No.9

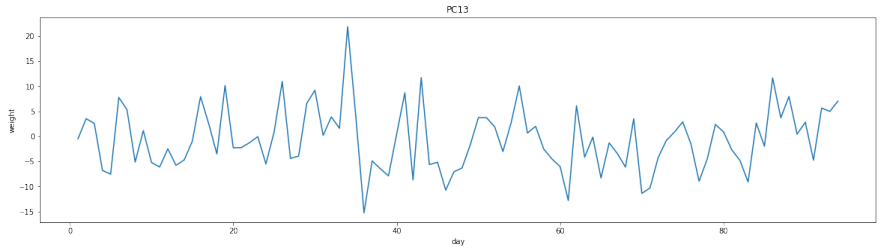

(b) Eigenface No.13

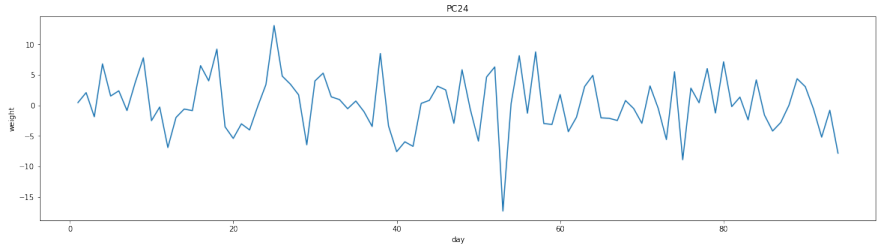

(c) Eigenface No.24

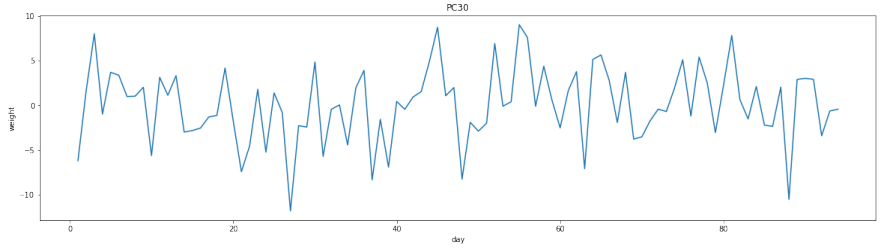

(d) Eigenface No.30

Figure 5.9: Weights of four eigenfaces of p3 in Figure 4.12

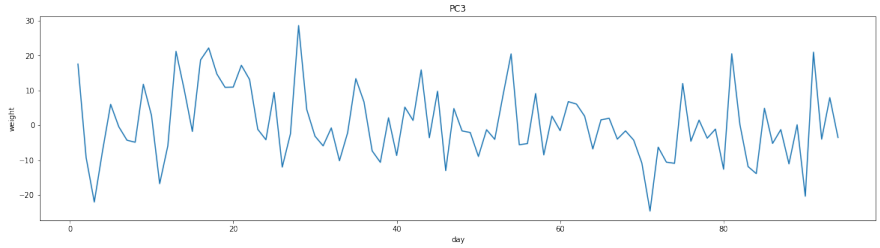

(a) Eigenface No.3

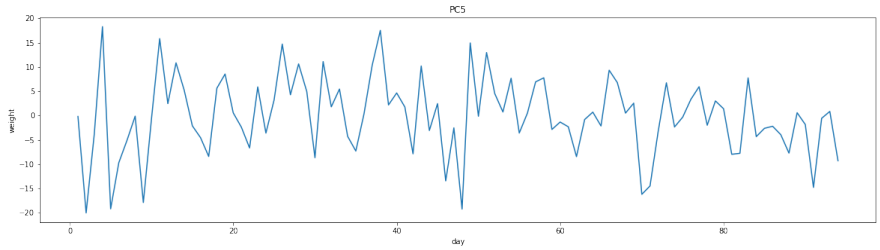

(b) Eigenface No.5

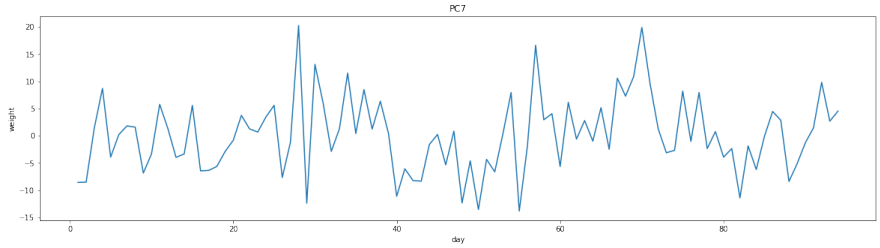

(c) Eigenface No.7

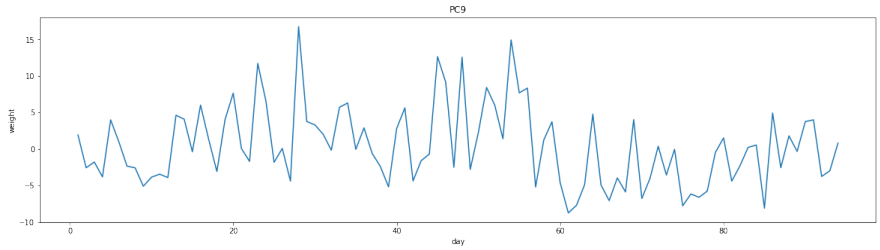

(d) Eigenface No.9

Figure 5.10: Weights of four eigenfaces of p3 in Figure 4.9

5.4 Summary

In this part, we will reconstruct some face images according to the time series analysis results discussed before, and the reconstructed face images of participant 1 and participant 2 at different times are shown in Figure 5.11.

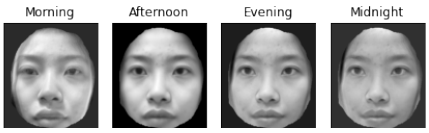

(a) Eigenface No.11 of p1

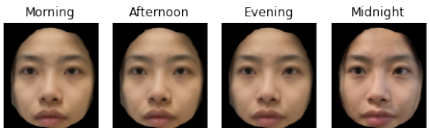

(b) Eigenface No.18 of p1

(c) Eigenface No.3 of p3

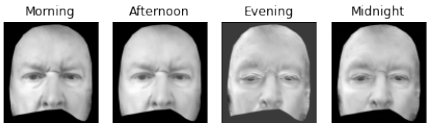

(d) Eigenface No.9 of p3

(e) Eigenface No.9 of p3

(f) Eigenface No.13 of p3

Figure 5.11: Some reconstructed face of p1, p3 at different times

According to the time analysis results and reconstructed images we get, we can conclude that:

- There are no obvious patterns visible over the full time period, and no obvious pattern when the data is grouped into 30-day month-like blocks.
- There appears to be some trends in the weights of some eigenvalues when grouped into four daily time blocks.
- From the reconstructed face, we can see that different person has different changes on their faces at different times. Participant 1 seems to be more pale and sleepy-eyed in the morning and looks energetic and rosy later in the day. Participant 2, on the contrary, looks more refreshed in the morning, and becomes tired as it gets later in the day.

Chapter 6

Conclusions

Overall, the eigenface method helps us to find some meaningful eigenfaces that represent some changes on the face, which include changes in the face contour, the skin tone, the shape of the bags under the eyes, the puffiness of the face, the depth of wrinkles, the colour of red areas on the cheek and so on.

The time series analysis showed that there is no sufficient evidence of periodic change patterns on the face. However, we can find some changes on the face at different times of the day. The time series analysis shows that the eyes are puffier in the morning, while the skin tone is rosier in the evening. But the results are not reliable enough because the standard deviations are usually very big in the analysis.

There are various possibilities why we cannot get the change patterns following the steps we use:

- The accuracy of face alignment is not high enough. Although the grey centroid and the mean face indicate that the performance of face alignment is reasonable, the eigenface method applied to the face images of the same person requires better face alignment.

- The masking step uses a single mask for each participant, which will cause part of the background to remain in the images after pre-processing. We should use a more accurate mask according to the face contour in the images for making.

- Interior factors of the images such as lighting conditions and resolution will also influence the analysis.

Future work should focus on the improvement of face alignment, masking, removing the unrelated factors (e.g. lighting conditions and resolution). We should try

other face alignment techniques and advanced analysis based on the eigenface method as well. Techniques such as deep learning can be involved in future work. Another suggestion is to use high dynamic range cameras instead of smart-phone cameras to capture more subtle effects.

Bibliography

[1] Paul Ekman. Facial expressions. *Handbook of cognition and emotion*, 16(301):e320, 1999.

[2] M Katsikitis and I Pilowsky. A study of facial expression in parkinson's disease using a novel microcomputer-based method. *Journal of Neurology, Neurosurgery & Psychiatry*, 51(3):362–366, 1988.

[3] Chaona Chen, Carlos Crivelli, Oliver GB Garrod, Philippe G Schyns, José-Miguel Fernández-Dols, and Rachael E Jack. Distinct facial expressions represent pain and pleasure across cultures. *Proceedings of the National Academy of Sciences*, 115(43):E10013–E10021, 2018.

[4] S. Gutta and H. Wechsler. Gender and ethnic classification of human faces using hybrid classifiers. In *IJCNN'99. International Joint Conference on Neural Networks. Proceedings (Cat. No.99CH36339)*, volume 6, pages 4084–4089 vol.6, 1999.

[5] Wen-Bing Horng, Cheng-Ping Lee, Chun-Wen Chen, et al. Classification of age groups based on facial features. *Journal of Applied Science and Engineering*, 4(3):183–192, 2001.

[6] Robin SS Kramer and Robert Ward. Internal facial features are signals of personality and health. *The Quarterly Journal of Experimental Psychology*, 63(11):2273–2287, 2010.

[7] M. A. Dabbah, W. L. Woo, and S. S. Dlay. Secure authentication for face recognition. In *2007 IEEE Symposium on Computational Intelligence in Image and Signal Processing*, pages 121–126, 2007.

[8] Wen-Bing Horng, Chih-Yuan Chen, Yi Chang, and Chun-Hai Fan. Driver fatigue detection based on eye tracking and dynamic template matching. In *IEEE Inter-*

national Conference on Networking, Sensing and Control, 2004, volume 1, pages 7–12. IEEE, 2004.

[9] Sachit Mahajan, Ling-Jyh Chen, and Tzu-Chieh Tsai. Swapitup: A face swap application for privacy protection. In *2017 IEEE 31st International Conference on Advanced Information Networking and Applications (AINA)*, pages 46–50, 2017.

[10] K. Ricanek and E. Boone. The effect of normal adult aging on standard pca face recognition accuracy rates. In *Proceedings. 2005 IEEE International Joint Conference on Neural Networks, 2005.*, volume 4, pages 2018–2023 vol. 4, 2005.

[11] In Cheol Jeong and Joseph Finkelstein. Introducing contactless blood pressure assessment using a high speed video camera. *Journal of medical systems*, 40(4):77, 2016.

[12] Xin Jin and Xiaoyang Tan. Face alignment in-the-wild: A survey. *Computer Vision and Image Understanding*, 162:1–22, 2017.

[13] Dmitri Bitouk, Neeraj Kumar, Samreen Dhillon, Peter Belhumeur, and Shree K Nayar. Face swapping: automatically replacing faces in photographs. In *ACM SIGGRAPH 2008 papers*, pages 1–8. 2008.

[14] Jason M Saragih, Simon Lucey, and Jeffrey F Cohn. Real-time avatar animation from a single image. In *2011 IEEE International Conference on Automatic Face & Gesture Recognition (FG)*, pages 117–124. IEEE, 2011.

[15] Ivan Gogić, Jörgen Ahlberg, and Igor S Pandžić. Regression-based methods for face alignment: A survey. *Signal Processing*, page 107755, 2020.

[16] Timothy F. Cootes, Gareth J. Edwards, and Christopher J. Taylor. Active appearance models. *IEEE Transactions on pattern analysis and machine intelligence*, 23(6):681–685, 2001.

[17] Timothy F Cootes, Christopher J Taylor, David H Cooper, and Jim Graham. Active shape models-their training and application. *Computer vision and image understanding*, 61(1):38–59, 1995.

[18] Ming Zhao, Chun Chen, S.Z. Li, and Jiajun Bu. Subspace analysis and optimization for aam based face alignment. In *Sixth IEEE International Conference on*

Automatic Face and Gesture Recognition, 2004. Proceedings., pages 290–295, 2004.

[19] Feng Jiao, Stan Li, Heung-Yeung Shum, and Dale Schuurmans. Face alignment using statistical models and wavelet features. In *2003 IEEE Computer Society Conference on Computer Vision and Pattern Recognition, 2003. Proceedings.*, volume 1, pages I–I. IEEE, 2003.

[20] Tong Wang, Haizhou Ai, and Gaofeng Huang. A two-stage approach to automatic face alignment. In *Third International Symposium on Multispectral Image Processing and Pattern Recognition*, volume 5286, pages 558–563. International Society for Optics and Photonics, 2003.

[21] Xin Miao, Xiantong Zhen, Xianglong Liu, Cheng Deng, Vassilis Athitsos, and Heng Huang. Direct shape regression networks for end-to-end face alignment. In *2018 IEEE/CVF Conference on Computer Vision and Pattern Recognition*, pages 5040–5049, 2018.

[22] Zhiwen Shao, Hengliang Zhu, Yangyang Hao, Min Wang, and Lizhuang Ma. Learning a multi-center convolutional network for unconstrained face alignment. In *2017 IEEE International Conference on Multimedia and Expo (ICME)*, pages 109–114. IEEE, 2017.

[23] Ian T Jolliffe. Principal components in regression analysis. In *Principal component analysis*, pages 129–155. Springer, 1986.

[24] Rajkiran Gottumukkal and Vijayan K Asari. An improved face recognition technique based on modular pca approach. *Pattern Recognition Letters*, 25(4):429–436, 2004.

[25] Hyun-Chul Kim, Daijin Kim, and Sung Yang Bang. Face recognition using the mixture-of-eigenfaces method. *Pattern Recognition Letters*, 23(13):1549–1558, 2002.

[26] Matthew Turk and Alex Pentland. Eigenfaces for recognition. *Journal of cognitive neuroscience*, 3(1):71–86, 1991.

[27] Dlib. Official website of Dlib. `http://dlib.net/`.

[28] Navneet Dalal and Bill Triggs. Histograms of oriented gradients for human detection. In *2005 IEEE computer society conference on computer vision and pattern recognition (CVPR'05)*, volume 1, pages 886–893. Ieee, 2005.

[29] Zhili Song, Shuigeng Zhou, and Jihong Guan. A novel image registration algorithm for remote sensing under affine transformation. *IEEE Transactions on Geoscience and Remote Sensing*, 52(8):4895–4912, 2013.

[30] Wang Xian, Ma Qinwei, Ma Shaopeng, and Wang Hongtao. A marker locating method based on gray centroid algorithm and its application to displacement and strain measurement. In *2011 Fourth International Conference on Intelligent Computation Technology and Automation*, volume 2, pages 932–935. IEEE, 2011.

[31] Lawrence Sirovich and Michael Kirby. Low-dimensional procedure for the characterization of human faces. *Josa a*, 4(3):519–524, 1987.